

Controllable Josephson current through a pseudo-spin-valve structure

C. Bell, G. Burnell, C. W. Leung, E. J. Tarte, D.-J. Kang, M. G. Blamire

*Materials Science Department,
IRC in Superconductivity and IRC in Nanotechnology,
University of Cambridge, United Kingdom*

(Dated: November 5, 2018)

A thin Co/Cu/Permalloy ($\text{Ni}_{80}\text{Fe}_{20}$) pseudo-spin-valve structure is sandwiched between superconducting Nb contacts. When the current is passed perpendicular to the plane of the film a Josephson critical current (I_C) is observed at 4.2 K, in addition to a magnetoresistance (MR) of $\sim 0.5\%$ at high bias. The hysteresis loop of the spin-valve structure can be cycled to modulate the zero field I_C of the junction in line with the MR measurements. These modulations of resistance and I_C occur both smoothly and sharply with the applied field. For each type of behaviour there is a strong correlation between shape of the MR loops and the I_C modulation.

PACS numbers: 74.50+r, 75.47.De, 85.25.Cp, 85.75.-d

Keywords: Josephson junction, pseudo-spin-valve

Josephson junctions with ferromagnetic barriers (SFS) have been investigated recently using weak ferromagnets. Due to the oscillating superconducting order parameter in the F layer, the groundstate phase difference of the S electrodes was found to change from 0 to π (a so-called π -junction) as a function of temperature and F thickness^{1,2}. SFS junctions have also been fabricated with the strong ferromagnets Ni^3 and Co^4 . In the above cases the F layer has a profound effect on the properties of the junction. Using an F layer to controllably alter the properties of a Josephson junction is important for a fundamental understanding of the physics, but also has potential applications as a memory element.

In this Letter we extend the work on single F layer junctions and examine a S/pseudo-spin-valve (PSV)/S Josephson junction. The PSV consisted of two F layers with different coercive fields, separated by a Cu spacer. This artificial structure allows active control of the magnetic state of the barrier. In contrast to previous relatively large SFS junctions where the F layer was demagnetised, here we actively pursue inhomogeneous magnetic structure. The magnetoresistance (MR) of the PSV gives direct access to information about relative orientation of the Co and Py layers, and the magnetic state of the barrier. The junction dimensions were such that the field H required to switch the F layers at 4.2 K is comparable to the $I_C(H)$ modulation period. The PSV structure with no antiferromagnetic pinning layer avoids the strong reduction of critical current density J_C found in for example γ -FeMn Josephson junctions⁵. We will show that I_C can be controlled by putting the PSV into the parallel and anti-parallel remanent states.

Nb/Py/Cu/Co/Nb films were deposited on (100) oxidised silicon substrates by d.c. magnetron sputtering at 0.5 Pa, in an in-plane magnetic field $\mu_0 H \sim 40$ mT. The sputtering system was cooled with liquid nitrogen and had a base pressure better than 3×10^{-9} mbar. The Nb thicknesses were 180 nm and Cu spacer thickness was 8 nm, (to avoid significant ‘orange peel’ magneto-static coupling between F layers). The Co and Py layers which

showed a Josephson current were of the order of 1 nm and 1.6 nm respectively. The films were patterned to micron scale wires with broad beam Ar ion milling (1 mAcm^{-2} , 500 V), and then processed with a Ga focused ion beam to achieve vertical transport with a device area in the range $0.2 - 1 \mu\text{m}^2$. The fabrication process is described in detail elsewhere⁶.

Transport measurements were made in a liquid He dip probe. For the $I_C(H)$ and $R(H)$ measurements a quasi-d.c. (~ 15 Hz) IV was directly measured and I_C extracted using a voltage criterion. The $R(H)$ measurements used a bias current of $2 - 3$ mA, which is much greater than I_C , but less than the critical current of the Nb electrodes. The magnetic field was applied in-plane in the direction of the applied field during deposition. As seen in the relatively thick device in Fig. 1, the $R(H)$ and $M(H)$ measurements are consistent with one another as expected. For the thinner F layers, Figs. 2 and 3 show the two different behaviours of $R(H)$. The sudden jumps in Fig. 3 compared to the smooth variation of R in Fig. 2 can be explained by sudden switches of a small number of domains in the barrier. The crossover from smooth to sharp $R(H)$ switching takes place as the junction area A is reduced below $\sim 0.45 \mu\text{m}^2$, but is not strongly dependent on the device aspect ratio, (the aspect ratio is the junction dimension perpendicular to the deposition field / dimension parallel to it). In both cases, despite the different $R(H)$ behaviour, $\text{MR} = (R_{\text{max}} - R_{\text{min}}) / R_{\text{max}}$ of the order of 0.5% was obtained for the devices in this work. The MR is consistent with the F layer and spacer thicknesses⁷. The $I_C(H)$ is not a ‘sinc’ function as seen in uniform junctions, and is hysteretic in the same sense as the MR measurements (inset of Fig. 2). In this case the junction dimension in direction perpendicular to the field is 320 nm. The first minima of the $I_C(H)$ pattern for this junction dimension with a non-magnetic barrier would be expected at $\mu_0 H \sim 60$ mT:⁵ hence there is extra complication added by the magnetic barrier.

To avoid this added complexity ‘zero field’ I_C was also measured. Hence the device was prepared in distinct

remnant states. To achieve this a saturating field of ± 30 mT was first applied. A field $\mp H_{\text{SET}}$, was then applied in the opposite direction. The field was then reduced to zero. The differential resistance as a function of bias current of the junction was then made with a lock-in amplifier, and the I_C found. In this way the parallel and anti-parallel remnant state I_C s were measured. Hence ‘applied field’ in Figs. 2 and 3 for the ‘zero field I_C ’ is H_{SET} . ‘ I_C ’ is the average of the absolute values of the positive and negative I_C s. The symbols in Figs. 2 and 3 show zero field I_C . The correlation between I_C and $R(H)$ is striking. The first sudden switch of $R(H)$ in Fig. 3 but not in I_C is attributed to a metastable state not present at zero field. For several devices $\Delta I_C = (I_C^{\text{max}} - I_C^{\text{min}}) / I_C^{\text{max}} \sim 30\%$, extremal values of 17% and 45% were also obtained, but there was no scaling with dimension, area or aspect ratio. The $I_C(T)$ monotonically decreased with T , with parabolic behaviour as $I_C \rightarrow 0$, (inset Fig. 2). When normalised to the I_C at 4.2 K both remnant states showed very similar behaviour: we attribute this to the T dependence of the superconducting gap. The

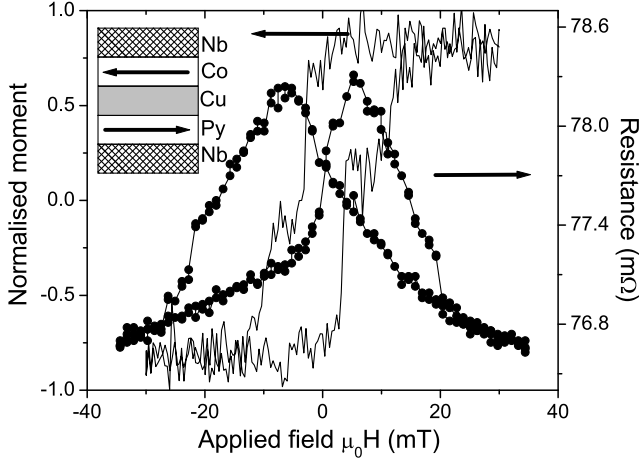


FIG. 1: Comparison of $M(H)$ loop at 30 K for a film with relatively thick F layers (2 nm Co and 3.2 nm Py), with a $R(H)$ measurement (symbols) at 4.2 K. MR $\sim 2\%$ in this case. Inset: schematic of the device (not to scale).

change in R , ΔR and R were inversely proportional to A (Fig. 4): hence interface scattering is the dominant mechanism of MR⁸. Current induced switching is not present since the current density is $\sim 1 \times 10^{10}$ Am⁻² which is a few orders of magnitude lower than required⁸. $A\Delta R$ was in the range $5.4 - 8.7 \times 10^{-17}$ Ωm^2 , and $AR = 1.1 \pm 0.2 \times 10^{-14}$ Ωm^2 . Using the two-current model from Yang et al⁹, with their ‘best fit’ parameters for Nb, Cu, Co and Py, for our thicknesses $AR = 9 \pm 1 \times 10^{-15}$ Ωm^2 in good agreement with our results. $A\Delta R$ was too small to predict within the errors of the parameters of Yang et al. The junction R_N is the same as the value of the $R(H)$ measurements, and will be referred to as simply R . The $I_C R$ was in the range 0.8 to 2 μV . The $I_C R$ for a given thickness of barrier should be constant.

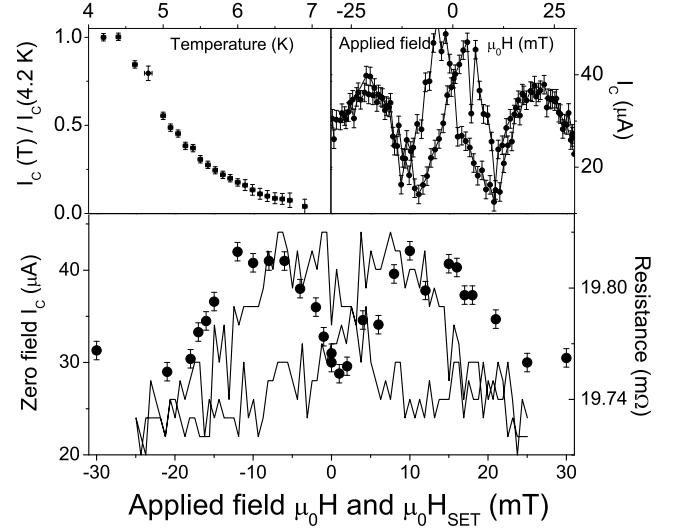


FIG. 2: Smooth variation of the zero field I_C (symbols) compared to $R(H)$ (solid line). Junction size was 950×570 nm. Left inset: $I_C(T)$ normalised to $I_C(4.2 \text{ K})$. Right inset: Hysteretic $I_C(H)$ for a 320×780 nm device.

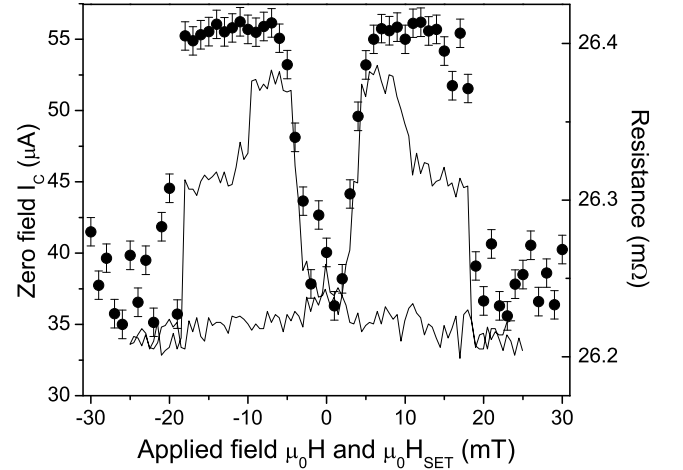


FIG. 3: Sudden jump of zero field I_C (symbols) compared to $R(H)$ (solid line). Junction is 600×730 nm.

Hence despite the apparent large difference in the shape of the $R(H)$, the $I_C R$ is the same to within a factor of approximately two, which is reasonable allowing for a few \AA variation of barrier thickness over the chip. Given that Co and Py are strong ferromagnets, we expect a small J_C , despite the thin barrier thickness. Compared to the Co junctions of Sürgers et al⁴, where the barrier thickness was 5 nm, J_C at 2.1 K was $\sim 1 \times 10^7$ Am⁻². Assuming $J_C \propto \exp(-d/\xi_F)$ with $\xi_F \approx 1$ nm, a thickness 2 nm gives $J_C \sim 2 \times 10^7$ Am⁻². Although the comparison is crude, the experimental values in the range $0.5 - 1.2 \times 10^8$ Am⁻² are somewhat larger than this. J_C is constant to within a factor of two over the range of areas, but showed an interesting scaling with device aspect ratio (inset of Fig.

4), which is not understood at present. The value of I_C and $R(H)$ behaviour with thermal cycling is not perfectly reproducible, but show the same qualitative behaviour. This is possibly due to different magnetic configurations ‘frozen in’ when cooled.

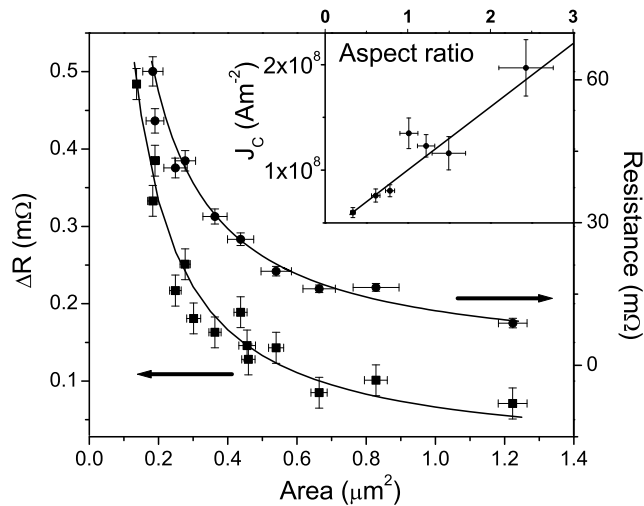


FIG. 4: Scaling of R and ΔR with A , lines are best fit to $1/A$ power law. Inset: scaling of J_C with aspect ratio.

With the device geometry stray flux from the electrodes is present⁶. However given the strong correlation between I_C and R for the two very different types of $R(H)$ behaviour, and that R is determined solely by magnetic structure of the barrier, we conclude that the effect of stray field from the electrodes is not important in directly determining I_C . A more quantitative argument can be used¹⁰: modelling the fringe field as a line source, the flux density $B = \mu_0 M_S d_F / 2\pi r$, where r is the distance from the end of the track, and d_F the F thickness. The saturation magnetisation $M_S = 1.42 \times 10^6 \text{ Am}^{-1}$ for Co. Considering the barrier as simply a 2 nm thick

Co, for $r = 500 \text{ nm}$, $B \sim 1 \text{ mT}$. The magnetic induction from the barrier itself must also be considered. Using a simplistic model, in the worst case if we assume all of the moment present in the barrier passes into the junction, perpendicular to the dimension x , then the flux in the junction is $\Phi = x d_F \mu_0 M_S$. For $x = 0.5 \mu\text{m}$, $\Phi \sim 0.8 \Phi_0$, ($\Phi_0 = h/2e$ is the flux quantum). This can explain the suppression of I_C , but not the lack of scaling of ΔI_C with the dimension x , and also neglects the ‘return flux’ in the opposite direction which should reduce Φ . Net magnetic induction shifts the $I_C(H)$ pattern away from zero field and reduces the zero field I_C ¹¹. Devices demagnetised both above and below T_C showed an increased value $R(0)$, above R_{max} as expected¹², but no increase in zero field I_C above I_C^{max} . Hence it would seem that stray induction does not strongly influence these devices.

In conclusion we have measured the Josephson current through a pseudo-spin-valve structure. The zero field I_C shows strong modulation as the distinct remanent states of the PSV were mapped out. There was a strong similarity between the $R(H)$ and zero field I_C . At present theoretical work has been done on similar structures^{13,14}, but in different limits to the present work. A combination of these works may be required to explain the complex behaviour due to the inhomogeneous magnetic structure in the PSV. It is nonetheless clear that I_C can be actively controlled using the PSV barrier. If the barriers are replaced by weaker F layers, (e.g. $\text{Cu}_x\text{Ni}_{1-x}$ or $\text{Pd}_x\text{Ni}_{1-x}$) then for $T < 4.2 \text{ K}$ a much larger J_C may be large enough to produce spin torque effects¹⁵. A suitable design with the weak alloys and thicknesses chosen to be around the $0 - \pi$ transition should allow the creation a controllable π -SQUID by switching one of the two devices into the anti-parallel state. This would be a magnetic version of the voltage controlled design using normal metal junctions¹⁶. We acknowledge the support of the Engineering and Physical Sciences Research Council, UK.

¹ V. V. Ryazanov, V. A. Oboznov, A. Y. Rusanov, A. V. Veretennikov, A. A. Golubov, and J. Aarts, Phys. Rev. Lett. **86**, 2427 (2001).
² T. Kontos, M. Aprili, J. Lesueur, and X. Grison, Phys. Rev. Lett. **86**, 304 (2001).
³ Y. Blum, A. Tsukernik, M. Karpovski, and A. Palevski, Phys. Rev. Lett. **89**, 187004 (2002).
⁴ C. Sürgers, T. Hoss, C. Schönenburger, and C. Strunk, J. Magn. Magn. Mater. **240**, 598 (2002).
⁵ C. Bell, E. J. Tarte, G. Burnell, C. W. Leung, D.-J.Kang, and M. G. Blamire, Phys. Rev. B (in press).
⁶ C. Bell, G. Burnell, D.-J.Kang, R. H. Hadfield, M. Kappers, and M. G. Blamire, Nanotechnology **14**, 630 (2003).
⁷ R. D. Slater, J. A. Caballero, R. Loloee, and W. P. Pratt Jr, J. Appl. Phys. **90**, 5242 (2001).
⁸ F. J. Albert, N. C. Emley, E. B. Myers, D. C. Ralph, and R. A. Buhrman, Phys. Rev. Lett. **89**, 226802 (2002).
⁹ Q. Yang, P. Holody, R. Loloee, L. L. Henry, W. P. Pratt

Jr., P. A. Schroeder, and J. Bass, Phys. Rev. B **51**, 3226 (1995).
¹⁰ T. W. Clinton and M. Johnson, J. Appl. Phys. **83**, 6777 (1998).
¹¹ V. V. Ryazanov, Usp. Fiz. Nauk **169**, 920 (1999).
¹² W. P. Pratt Jr, S.-F. Lee, J. M. Slaughter, R. Loloee, P. A. Schroeder, and J. Bass, Phys. Rev. Lett. **66**, 3060 (1991).
¹³ F. S. Bergeret, A. F. Volkov, and K. B. Efetov, Phys. Rev. B **64**, 134506 (2001).
¹⁴ N. M. Chtchelkatchev, W. Belzig, and C. Bruder, JETP Lett. **75**, 646 (2002).
¹⁵ X. Waintal and P. W. Brouwer, Phys. Rev. B **65**, 054407 (2002).
¹⁶ J. J. A. Baselmans, B. J. van Wees, and T. M. Klapwijk, Appl. Phys. Lett. **79**, 2940 (2001).